Research Paper

EERI EARTHQUAKE SPECTRA

Impact of modeling decisions on seismic loss and fragility assessment of steel buildings

Earthquake Spectra
1–24

DOI: 10.1177/87552930251360751
journals.sagepub.com/home/eqs
Sage

Shivalinga Baddipalli, M. EERI[1], Roberto Gentile, M. EERI[2], Gerard J O' Reilly, M. EERI[3], Davit Shahnazaryan[3], and Mohsen Zaker Esteghamati, M. EERI[1]

Abstract

Seismic loss estimation is an essential tool for assessing the performance and resilience of buildings exposed to seismic hazards. Numerous loss methodologies with varying fidelities exist, with each comprising different steps and requiring analysts to adopt certain modeling decisions and assumptions. This study compares three seismic loss estimation methods, namely FEMA P-58 component-, story loss function (SLF)-, and HAZUS assembly-based approaches, using a database of 621 steel special moment-resisting frame buildings with diverse designs and geometries. In addition, a set of sensitivity analyses are performed to evaluate the influence of key modeling decisions in fragility and loss assessment stages on different loss methodologies. These decisions include (1) intensity measure-engineering demand parameter (IM-EDP) formulation to derive fragility functions, (2) EDP proxy for fragility models within the assembly-based method, (3) characterization of demolition fragility, and (4) uncertainties in nonstructural component quantities. The results show that the assembly-based approach estimates lower median loss for short- to medium-rise buildings but higher estimates for taller ones, with significantly higher variability in losses for multi-story buildings compared to the component-based approach. In contrast, the SLF-based method yields slightly higher median loss for 1-story buildings but consistently lower estimates for multi-story buildings than the component-based approach. The sensitivity analysis highlights that the critical modeling decisions vary by the selected method. The assembly-based approach shows greater sensitivity to the choice of EDP proxy impacting the dispersion of losses. In contrast, uncertainties in nonstructural component

[1]Department of Civil and Environmental Engineering, Utah State University, Logan, UT, USA
[2]Department of Risk and Disaster Reduction, University College London, London, UK
[3]Centre for Training and Research on Reduction of Seismic Risk (ROSE Centre), Scuola Universitaria Superiore IUSS Pavia, Pavia, Italy

Corresponding author:
Mohsen Zaker Esteghamati, Department of Civil and Environmental Engineering, Utah State University, 4110 Old Main Hill, Logan, UT 84322, USA.
Email: mohsen.zaker@usu.edu

quantities predominantly govern both the median and dispersion of losses for the component-based approach, and the selected IM-EDP formulation has the highest effect on SLF-based estimates.

Keywords
Seismic loss estimation, FEMA P-58 component-based method, HAZUS assembly-based approach, story loss function, sensitivity analysis

Date received: 12 December 2024; accepted: 4 July 2025

Introduction

Seismic loss analysis is an essential tool in assessing and improving the performance and resiliency of buildings against future earthquakes and disaster risk reduction. Nevertheless, various seismic loss methodologies exist in the literature (Calvi et al., 2006), ranging from detailed methods, such as the FEMA P-58 (FEMA P-58-1, 2012, FEMA P-58-1, 2018) component-based approach, to simplified methods, namely the HAZUS (Hazards U.S.) assembly-based approach (HAZUS-MH 2.1, 2015). In the 1990s, driven by the interest of insurance industries, FEMA developed the HAZUS seismic loss estimation method primarily for regional assessments. However, the accompanying advanced engineering building module also allowed building-level assessments (Kircher et al., 1997, 2006). Initially, HAZUS focused on empirical methods leveraging past earthquake data to generate vulnerability functions and damage probability matrices based on the framework by FEMA (1999) and Whitman et al. (1997). Later, HAZUS' scope was broadened beyond earthquake hazards, including floods (Scawthorn et al., 2006), hurricanes (Kijewski-Correa et al., 2023), and tsunamis (Frucht et al., 2021), advancing into HAZUS-Multi-Hazard (HAZUS-MH) (Schneider and Schauer, 2006). In HAZUS-MH 2.1, the structural response, damage, and repair costs are evaluated using building capacity curves, fragility functions, and repair cost ratios, respectively, based on the building's lateral force resisting system, height, degree of code compliance, and occupancy among other user-defined parameters. The structural responses are determined based on the capacity spectrum method by idealizing the multi-degree-of-freedom as a single-degree-of-freedom system.

Although the HAZUS assembly-based method allows for rapid loss estimation across large building portfolios, it does not capture the unique characteristics of structural and nonstructural components of a given building (Ramirez et al., 2012). Therefore, the FEMA P-58 methodology was developed as a framework for building-specific loss estimation to integrate hazard analysis, structural response, and damage estimation (Baker and Cornell, 2008; Cornell and Krawinkler, 2000). Nonetheless, it is data- and effort-intensive, which renders this method unfeasible for rapid assessments of large building portfolios (Porter et al., 2015) or the early design phases as detailed information for specific components was often unavailable (Esteghamati et al., 2023; Esteghamati and Flint, 2021; Ramirez and Miranda, 2009). To address these shortcomings, the story loss function (SLF) approach was developed to aggregate losses of all the components in a specific group of damageable elements (e.g. deformation-sensitive nonstructural components) in a story for a known value of structural demand. Ramirez and Miranda (2009) pioneered SLFs to relate engineering demand parameters (EDPs) directly to economic losses (decision variables, or DVs) at the story level, generally referred to as EDP-DV functions. This method simplifies the loss estimation process by using predefined loss functions that describe repair costs for a range of building types and damageable components (O'Reilly, 2019; O'Reilly and Shahnazaryan, 2024; Papadopoulos et al., 2019; Ramirez, 2009; Shahnazaryan et al., 2021; Shahnazaryan, and O'Reilly, 2021; Welch et al., 2014).

While various loss assessment methods with different fidelities have been proposed, the extent of difference in their estimates is not well understood. Limited studies compared component- and SLF-based methods (Papadopoulos et al., 2019; Shahnazaryan et al., 2021) and component-based and HAZUS methodology (Cremen and Baker, 2021), where the scope of such studies has been limited to a few archetype buildings. For example, Papadopoulos et al. (2019) compared component-based and SLF-based methods using a single 4-story steel moment-resisting frame building, whereas Shahnazaryan et al. (2021) compared the two methods using a 3-story reinforced concrete (RC) school building. They demonstrated that SLF-based methods provide results comparable (slightly higher) to the more detailed component-based approach, where the difference was about 9%. Meanwhile, Cremen and Baker (2021) evaluated the FEMA P-58 component-based approach against the HAZUS methodology for two 7- and 14-story buildings and showed that the range of mean loss ratio from the FEMA P-58 method is larger than HAZUS across different lateral systems, buildings' ages, and occupancies. However, the range of mean loss ratio estimated by HAZUS for steel moment frames is higher than the FEMA P-58 method. Nevertheless, since these studies focused on a limited set of archetype buildings, questions remain on the generalizability of their results for building portfolio assessments.

These existing loss methodologies include several analysis steps (e.g. hazard analysis, damage analysis), where the methodological choices at each step can significantly affect the estimated loss (Baker and Cornell, 2008; Crowley et al., 2005; Silva et al., 2019; Zaker Esteghamati, 2022). However, the literature has mostly focused on the impact of hazard analysis, ground motion (GM) selection, building's age, occupancy, and lateral system (Cremen and Baker, 2021; Dyanati et al., 2017; Lamprou et al., 2013; Porter et al., 2002; Silva et al., 2020), leaving the impact of different decisions on fragility and loss analyses on seismic loss assessment underexplored. For instance, Porter et al. (2002) evaluated a 7-story nonductile RC moment frame building and investigated the impact of GM and building characteristics on repair cost uncertainty. Lamprou et al. (2013) analyzed the effect of seismic hazard and component-level damage uncertainties on life-cycle repair costs for a 4-story RC moment frame building. Dyanati et al. (2017) explored the influence of GM selection on expected annual losses (EALs) for a 6-story braced steel frame building. Silva et al. (2020) examined the impact of brace-to-frame connection modeling strategies on seismic loss estimates for steel concentrically braced frames. Finally, Cremen and Baker (2021) conducted a variance-based sensitivity analysis to study how building age, occupancy, and lateral system affect loss estimates. Overall, the varying scope and the multitude of methodological choices hinder a broader interpretation of results, where such issues exacerbate decisions that are not typically included in these sensitivity assessments.

This research presents a systematic comparison of FEMA P-58 component-, SLF-, and HAZUS assembly-based loss assessment methods over a comprehensive building inventory of 621 steel moment-resisting frames (SMRF) with varying designs and geometries. The main objective of this article is to quantify the extent to which the estimates from different loss methodologies vary and investigate how such differences can be reduced through modeling assumptions. Therefore, sensitivity analyses are performed to evaluate the impact of various underexplored decisions at fragility and loss analysis stages on the estimated loss, providing guidance on improving consistency between estimates from different methodologies. Specifically, this study investigates the effect of the analyst's choices for (1) mathematical formulations of intensity measure-engineering demand parameter (IM-EDP) relationship, (2) the EDP representation in damage models within the assembly-based method, (3) nonstructural quantities uncertainties, and (4) demolition loss modeling. This article is structured as follows: section "Description of steel building database" describes the steel building database used in the study. Section "Loss assessment methodology" discusses the methodology adopted for component-, SLF-, and assembly-based seismic loss estimation. Section "Comparison of seismic loss estimates from assembly-, SLF-, and component-based approaches" compares the results from the discussed loss assessment methods, followed by a detailed sensitivity analysis in section "Sensitivity of seismic loss estimates to modeling decisions." Section "Discussion of results and recommendations" compares the relative importance of different analysis decisions considered across all different methodologies and provides necessary recommendations. Finally, section "Conclusion" summarizes the findings of the study and limitations with future work.

Description of steel building database

This study considers a database of 621 steel moment-resisting frame buildings, which provide seismic designs, nonlinear finite element models, the GM suite, and seismic responses (Guan et al., 2021). The database includes 1-, 5-, 9-, 14-, and 19-story buildings with a typical story height of 13 *ft* and varying first story heights of 13 *ft*, 19.5 *ft*, and 26 *ft*. The typical floor consists of 5 bays in both longitudinal and transverse directions. Special moment-resisting frames are located at the building perimeter, with the number of bays varying between 1, 3, and 5 in each orthogonal direction. The bay widths are 20 *ft*, 30 *ft*, and 40 *ft*, respectively. The buildings were designed for the high seismic zone in Los Angeles, California (Site class D), with spectral acceleration values of $S_s = 2.25\ g$ and $S_1 = 0.6\ g$.

The database also provides two-dimensional nonlinear models of these buildings developed in OpenSees (McKenna et al., 2000). The material nonlinearity in the beams and columns was captured using a concentrated plasticity approach with plastic hinges assigned at both ends of the members. These hinges were modeled as zero-length rotational springs using the modified Ibarra–Medina–Krawinkler (IMK) material model (Ibarra et al., 2005; Ibarra and Krawinkler, 2005; Lignos and Krawinkler, 2011), which simulates hysteretic behavior incorporating strength and stiffness deterioration effects. In addition, the cyclic deterioration effects (basic strength, post-capping strength, and unloading stiffness) are considered following empirical relationships from past studies (Ibarra and Krawinkler, 2005; Lignos, 2008; Lignos and Krawinkler, 2011). Finally, the shear yielding in the beam-column joints was modeled using the panel zone formulation developed by Krawinkler (1978), which captures parallelogram-shaped deformations through a combination of elastic beam-column elements and zero-length rotational springs, including a trilinear rotational spring at one corner to simulate shear distortion.

Geometric nonlinearity was introduced by considering the P-delta effect through a leaning column connected to the frame through truss element. Consequently, this approach only captures P-Δ effects and does not explicitly account for the stiffness and strength contributions of the gravity frame (Gupta and Krawinkler, 1999). A damping ratio of 2% was assigned to the first and third modes of all frames. Nonlinear time history analyses of the models were conducted using a suite of 240 GMs recorded from 12 past seismic events in California (Miranda, 2000). The magnitude of GMs ranges between 6.0 and 7.0, and their peak ground acceleration is between 0.03 g and 0.61 g. The analysis results were post-processed, and different EDPs, such as peak inter-story drift ratio (PIDR), peak floor acceleration (PFA), and residual inter-story drift (RIDR, referred to as residual drift for brevity), were captured. Further detailed procedures regarding numerical modeling, structural designs, GMs, and structural responses of the database buildings can be found in Guan et al. (2021).

Loss assessment methodology

Figure 1 illustrates the overall methodology for loss comparison. The estimated seismic response, including PIDR, PFA, and RIDR, was collected from the database described in the previous section (Guan et al., 2021). This response database was then used to perform fragility and loss analyses, as will be described next. Table 1 summarizes the assumptions and methodological choices for all the performed loss analyses. Additional information on the mathematical formulation of different loss assessment methodologies can be found in Appendix 1.

For all different methods, the final loss estimates are presented in terms of the EAL, which is defined as the average annual economic loss anticipated due to earthquake-induced damage. To derive EAL, the conditional expectation of losses given IM is multiplied by the seismic hazard curve and numerically integrated over the range of IMs. The mean annual frequency of exceedance of IM (λ_{IM}) for all the possible IMs at the site of interest as described by seismic hazard curves is shown in Figure 2. The seismic hazard curves were obtained using the USGS Unified Hazard Tool (United States Geological Survey, 2023) for a site in Los Angeles (334.008°N, 118.152°W). Figure 2 shows the seismic hazard curves for spectral acceleration (S_a) at fundamental periods of 0, 0.1, 0.5, 1, and 2 s. For database buildings with fundamental periods not explicitly shown, the seismic hazard curves are interpolated using the curves provided in Figure 2.

FEMA P-58 component-based loss assessment

The methodology proposed by Ramirez and Miranda (2012) was used to calculate component-based seismic losses. The component fragility and cost functions for structural (IDR-S), nonstructural drift sensitive (IDR-NS), and nonstructural acceleration-sensitive (PFA-NS) components (i.e. median and dispersion of $P\left(DS_{ij}|EDP_k\right)$ and $E\left(L_{ij}|DS_{ij}\right)$ in Equation (A.2) in Appendix 1) were taken from P-58 inventories (FEMA P-58-3, 2018). The component quantities were calculated using the FEMA P-58 Normative Tool (FEMA P-58-1, 2018). Table S1 in Supplementary Materials provides the quantity, fragility, and repair cost functions of the damageable components considered in this study for a sample 5-story case study building. It should be noted that while the fragility parameters of building components are the same for the entire building database, the components' quantities and the median repair cost vary with the building geometry, namely, the number of stories and bays, bay width, and number of SMRF bays. The median repair cost value depends on the quantity of components and follows a linear relationship, where the median repair cost decreases as the quantity increases. Moreover, the total replacement cost for all buildings in the database is assumed to be $250 per square foot (Terzic et al., 2012).

The quantity of nonstructural components varies based on the floor area and occupancy type, where the occupancy type was assumed as an office. For IDR-NS components, three quantity cases exist in the database, corresponding to floor areas of 10,000 ft^2, 22,500 ft^2, and 40,000 ft^2. Similarly, floor-level PFA-NS components show three quantity cases based on floor area, whereas fifteen unique quantity cases are present for building-

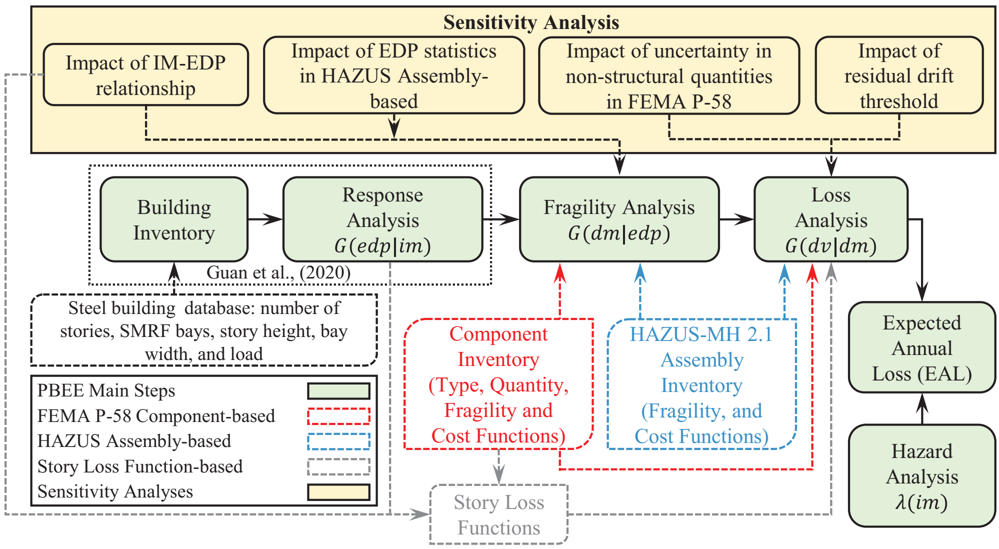

Figure 1. Comparison and sensitivity analysis of seismic loss assessment methodologies.

level PFA-NS components based on the existing number of stories and typical floor areas in the database. For IDR-S components, the column base plates were assumed to be present at the bottom of the SMRF frames, and their quantity was determined based on the number of SMRF columns. Column splices were considered at every alternate floor level in all the columns (Hwang et al., 2019; Hwang and Lignos, 2017). In addition, one-sided or two-sided reduced beam section (RBS) connections were considered depending on the number of SMRFs for frame connections. Finally, shear tabs were assumed at two ends of the gravity beams at each floor level, where the quantity of corrugated slab was determined based on the floor area.

HAZUS assembly-based loss assessment

The assembly-based approach (HAZUS-MH 2.1, 2015, Esteghamati and Farzampour, 2020) aggregates components' loss in terms of IDR-S, IDR-NS, and PFA-NS assemblies. Herein, the regression is performed between a representative building-level response (often taken as maximum EDP over all floors) and IM to characterize $P(EDP|IM)$ distribution. The fragility and cost functions of IDR-S, IDR-NS, and PFA-NS assemblies (i.e. median and dispersion of $P\left(DS_{aj}|EDP\right)$ and $E\left(L_{aj}|DS_{aj}\right)$ in Equation (A.3) in Appendix 1) were taken from HAZUS-MH 2.1 (2015), and their values are shown in Tables S2 and S3 in Supplementary Materials. In addition, dispersion values of 0.4, 0.5, and 0.6 were considered for IDR-S, IDR-NS, and PFA-NS assemblies. Finally, $P(D|NC, IM)$, $E[L_T|IM]$, and EAL were calculated using a similar procedure described in FEMA P-58 component-based loss assessment (Appendix 1).

SLF-based loss assessment

SLF represents the aggregated loss of all the damageable components present in a specific story with respect to the EDP level. Generally, SLFs are developed separately for a group

Table 1. Parameters and assumptions for loss estimation methodologies

Parameter/Assumption	FEMA P-58 component-based method	SLF-based method	HAZUS assembly-based method
Fragility and cost functions	FEMA P-58 component fragility and cost functions (FEMA P-58-1, 2012)	FEMA P-58 component fragility and cost functions (FEMA P-58-1, 2012)	HAZUS assembly-level fragility and cost functions (HAZUS-MH 2.1, 2015)
Correlation of EDPs	Not considered	Not considered	Not considered
Correlation of components	Not considered	Not considered	Not applicable
Damage state definitions	Explicit damage states for each component	Aggregated damage states for component groups within the same story	Assembly-level damage states
Level of modeling detail	Highest[a]	Moderate[b]	Lowest[c]
EDP representation	Floor-level EDPs	Floor-level EDPs	Building-level EDPs
Aggregation method	Component level	Story level	Assembly level
Quantities for components/assemblies	Median quantities	Median quantities	Implicit assumptions on quantities
Uncertainty in damage states and repair costs	Probabilistic damage states with median repair costs	Explicitly considered	Probabilistic damage states with median repair costs

[a]Evaluates each component individually across all stories.
[b]Aggregates components at the story level using SLFs.
[c]Evaluates assemblies without distinguishing individual components.

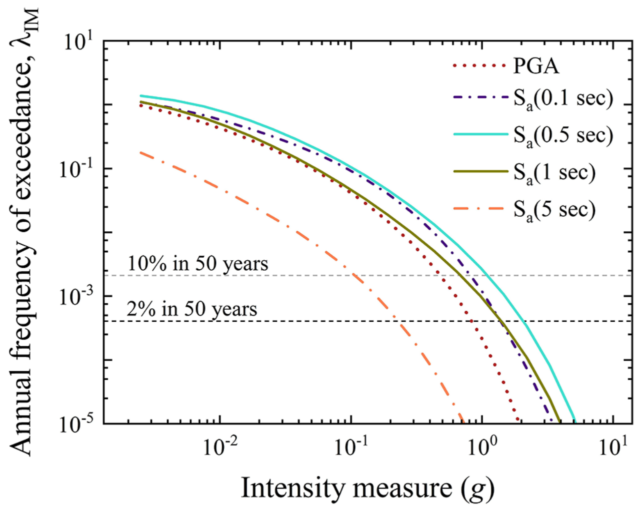

Figure 2. Seismic hazard curves for intensity measure at different building periods.

of specific components present in a story for IDR-S, IDR-NS, and PFA-NS assemblies based on the detailed inventory of building components (Shahnazaryan et al., 2021). The same component inventory described in the FEMA P-58 loss assessment section (Table S1 of Supplementary Material) was used to generate SLFs. These components were then grouped based on their EDP sensitivity to develop SLFs for different assemblies, referred to as performance groups in the SLF methodology.

In this study, SLFs were developed to address the variations in component distribution across different building configurations. Figure 3 presents SLFs developed for IDR-S, IDR-NS, and PFA-NS components. As shown in Figure 3, for IDR-S components, three SLFs were generated for column base plates corresponding to each SMRF bay in the plan, and an additional SLF was created for column splices. Meanwhile, nine SLFs were created for the remaining components—shear tabs, one-sided and two-sided RBSs, and slabs—considering different combinations of the number of SMRF bays and bay widths of the building. For IDR-NS and PFA-NS floor-level components, three SLFs were developed for three different bay widths. Furthermore, fifteen SLFs were developed for PFA-NS building-level components for fifteen different combinations of story numbers and bay widths. The SLF combination choices were driven by the necessity of capturing all possible combinations of SMRF bays and bay widths for each building for given EDPs. Further details regarding the development of SLFs can be found in Shahnazaryan et al. (2021) and Papadopoulos et al. (2019).

Comparison of seismic loss estimates from assembly-, SLF-, and component-based approaches

Figure 4 presents the normalized EAL values estimated by the three loss methodologies for the entire steel building database. Overall, the assembly-based approach yields lower median EALs for short- to medium-rise buildings but larger estimates for taller structures. Conversely, the SLF-based method provides higher EALs for 1-story buildings but lower estimates for medium- to high-rise structures than the component-based approach. This

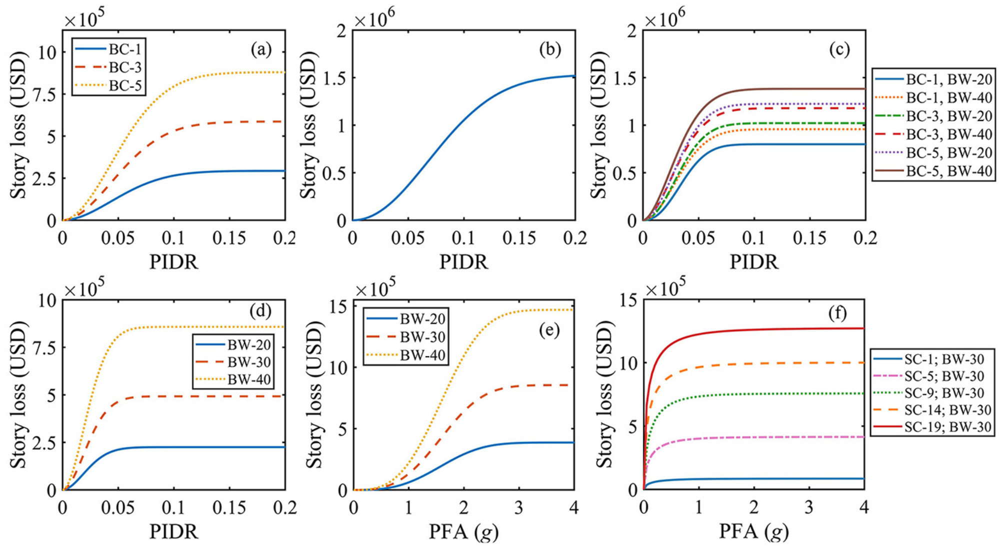

Figure 3. Story loss functions (SLFs) of steel database buildings for (a) column base plates for three SMRF bays count (BC), (b) column splices for 36 columns, (c) four remaining IDR-S components for only a few out of nine combinations of BC and bay widths (BW), (d) four IDR-NS components for three BW, (e) twelve floor-level PFA-NS components for three BW, and (f) five building-level PFA-NS components for only a few out of 15 combinations of story count (SC) and BW.

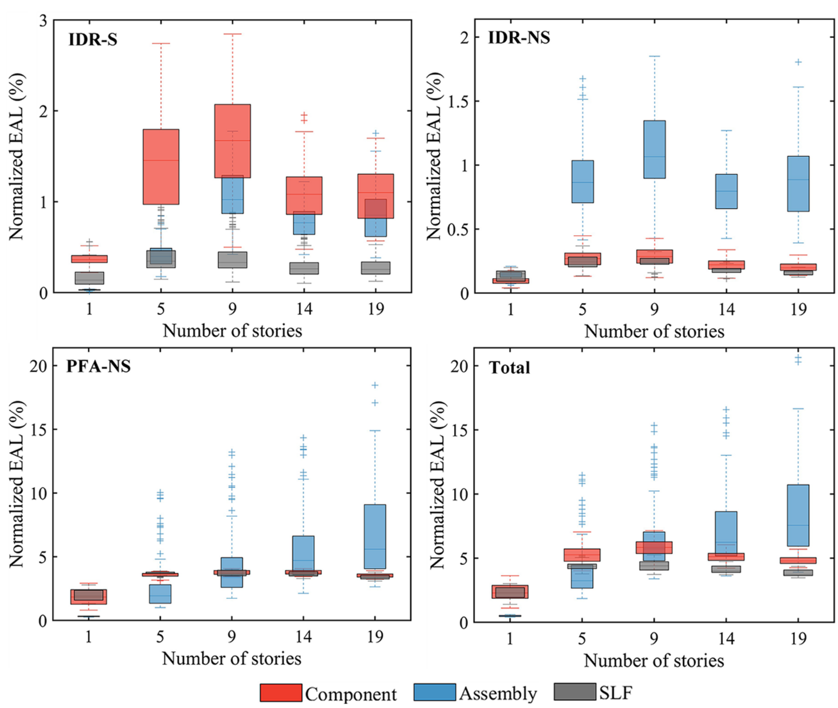

Figure 4. Normalized EAL (in % of replacement cost) of steel database buildings of different considered loss methodologies for (a) IDR-S, (b) IDR-NS, (c) PFA-NS, and (d) total loss assemblies.

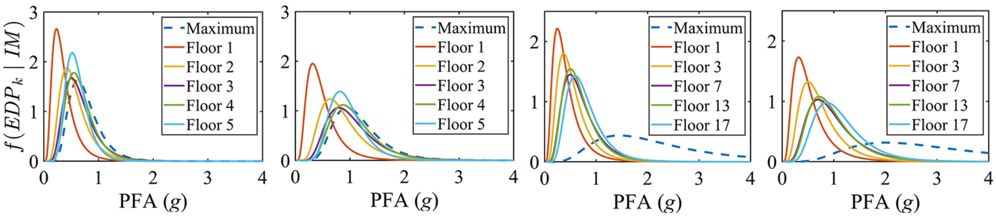

Figure 5. Probability density function of PFA at the *k*th floor (i.e. EDP_k) and maximum PFA given *IM* for a sample for (a) IM = 0.5 g and (b) IM = 1 g for a sample 5-story building, (c) IM = 1.5 g and (d) IM = 2 g for a sample 9-story building.

trend can be attributed to the difference in how each method captures building damage and the cost functions of corresponding damage states. For example, taller buildings typically experience higher PFA demands, which lead to higher estimated damage. Since HAZUS uses significantly higher repair cost ratios (compared to other methods) for higher damage estimates (Table S3), it provides larger EALs for taller buildings. In contrast, short- to medium-rise buildings experience lower PFA demands, which fall within lower damage states, where HAZUS uses more conservative cost ratios, thus resulting in lower EALs. Since total loss is mostly governed by nonstructural acceleration-sensitive losses, the same patterns are observed for total loss estimates. For example, the median values of total EAL obtained from the assembly-based approach are 22% and 58% higher for 14- and 19-story buildings and 79%, 39%, and 2% lower for 1-, 5, and 9-story buildings compared to the component-based method, respectively. On the other hand, the median EAL values from the SLF-based approach are 0.44% higher for 1-story buildings and 17%, 25%, 22%, and 22% lower for 5-, 9-, 14-, and 19-story buildings compared to the component-based approach, respectively. This difference is due to that the SLF-based method involves sampling of both damage states and repair costs to derive loss for a given EDP value. In contrast, the applied component-based method ignores the uncertainty in repair costs, leading to higher loss estimates. The difference between SLF- and component-based losses for shorter buildings of this study is similar in magnitude (about 1% difference) to the previous study by Shahnazaryan et al. (2021), albeit they found the former method to provide higher losses. This discrepancy could be attributed due to differences in the building inventory, structural systems, designs, and geometries between the two studies.

Comparing the dispersion in the total EAL estimates, the assembly-based method exhibits significantly higher variability than component-based as building height increases. Over the entire database, the dispersion of the total EAL computed by the assembly-based method is 3 times larger than the component-based method, respectively. This is primarily due to larger uncertainty in capturing structural response distribution using a single proxy (maximum EDP over the entire building) in the assembly-based method. As shown in Figure 5, there is a larger variability for maximum PFA response particularly for taller buildings, as compared to maximum floor-level PFA (used in component- and SLF-based approaches). In addition, HAZUS fragility functions have higher variability (especially for moderate to complete damage states in Table S2) and, when convoluted with more spread EDP distributions, amplify the variability in computed losses.

Comparing loss methods across different assemblies, PFA-NS losses follow a similar trend to the total loss. For IDR-NS losses, the assembly-based approach consistently estimates significantly higher EAL median values for all the database buildings. This observation stems from the higher repair cost ratios assigned in HAZUS, relative to other methods, for extensive to complete damage states (Table S3), which are triggered by the building's maximum PIDR response. On the contrary, the difference between median losses from SLF- and component-based methods remains similar, with a maximum difference of 20% for multi-story buildings. Finally, for the IDR-NS losses, both the assembly- and SLF-based methods provide significantly lower median values of EAL across entire building heights than the component-based method. The difference between median structural loss from component- and assembly-based ranges from 23% to 92%, where this range changes to 61%–80% when comparing SLF- and component-based methods. This is because, collectively, repair cost ratios for structural components from FEMA P-58 (Table S3 in Supplementary Material) are higher compared to the aggregated values used in HAZUS (Table S3 in Supplementary Material). As a result, structural losses derived from the component-based method are consistently higher than those from SLF and HAZUS across all building heights.

Sensitivity of seismic loss estimates to modeling decisions

Several modeling decisions related to fragility and loss assessment were studied in the sensitivity analysis (Figure 1). These decisions were selected as they are often left to the analyst's judgment, and since no proper guidance exists in the literature, this subjectivity can result in inconsistencies, even when structural responses and hazard data are derived consistently. As shown in Figure 1, the sensitivity analysis for fragility-related decisions includes (1) the effect of different methods of constructing IM-EDP mathematical relationships, namely linear and bilinear models across all loss methods; (2) the impact of EDP representation through a single statistic (e.g. maximum, mean, weighted average of different EDP statistics) in the assembly-based approach. Similarly, two modeling choices were investigated for the loss analysis stage: (1) the impact of residual drift threshold on demolition loss and (2) the impact of uncertainty in nonstructural quantities. For each sensitivity assessment, loss analyses are repeated by varying the parameter of interest and maintaining all other assumptions consistent with the previous section.

Impact of IM-EDP relationship on loss models

Previous research (Freddi et al., 2017, O'Reilly & Monteiro, 2019; Tubaldi et al., 2016) has highlighted the importance of bilinear EDP-IM models in accurately capturing structural behavior, such as yielding, cracking, nonductile mechanisms, and other inelastic phenomena, particularly for PFA response. Therefore, this sensitivity assessment evaluates how the IM-EDP model to capture different regions of structures behavior (e.g. through a bilinear model) influences the loss estimates compared to the conventional linear IM-EDP models. Figure 6 compares the total normalized EAL estimated using two different IM-EDP mathematical models, namely, linear and bilinear models. Table S4 of Supplementary Materials also presents the median and dispersion of normalized EAL using three loss methodologies across various assemblies for linear and bilinear IM-EDP relationships. Here, linear models followed the conventional approach of fitting a linear regression in the logarithmic space, whereas the bilinear model was fitted to IM-EDP data by dividing the data into two linear segments at a "*breakpoint*," where linear regressions were performed separately for each segment. An iterative algorithm was developed to identify the location of the breakpoint to minimize the sum of squared residuals for each

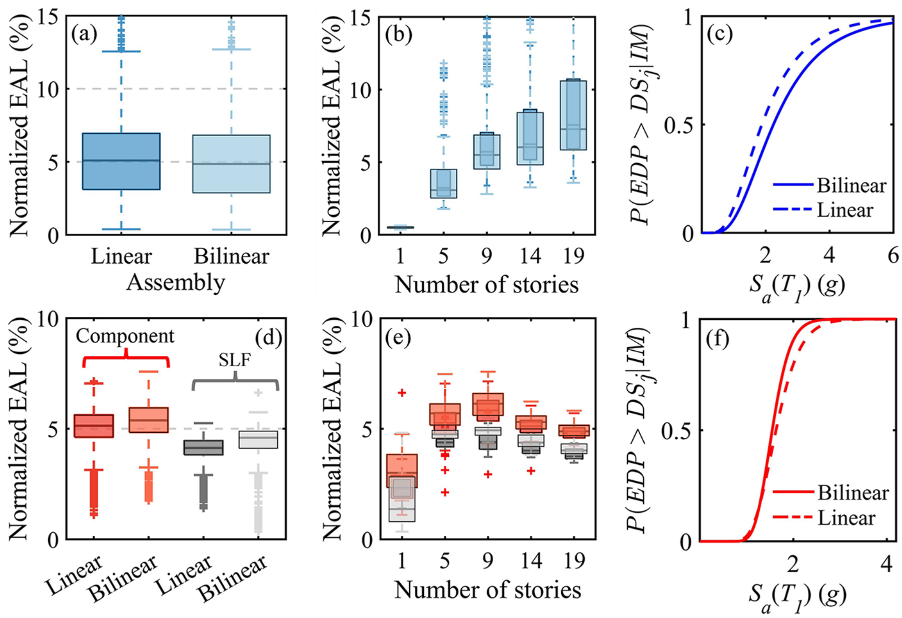

Figure 6. Normalized total EAL (in % of replacement cost) of steel buildings for linear and bilinear IM-EDP relationships across three methodologies and number of stories. Subplots (a) and (d) compare EAL distributions for assembly-, component-, and SLF-based methods, respectively, while (b) and (e) show EAL distributions across various buildings with different number of stories, (c) and (f) present the probability of exceeding complete damage state given $S_a(T_1)$, contrasting linear and bilinear relationships.

segment. The algorithm would then adjust the line segments to ensure the continuity of the fitted model. Figure 7a to d shows sample bilinear and linear models used for a 14-story building across different loss methodologies. In addition, Figure 6c and f presents the fragility curves for the same building for a complete damage state threshold. As shown in Figure 7a to d, the bilinear model can more accurately capture the changes in response at high IM values compared to a linear model.

As shown in Figure 6a, the difference between bilinear and linear IM-EDP models is negligible for the assembly-based approach, where the bilinear model provides 5% lower median loss than a linear model. In addition, Figure 6b demonstrates that this trend remains the same among all building heights. This is mainly due to the linear model over-predicting the maximum building-level EDP response at higher IM values compared to the bilinear relationship, resulting predicting higher damage states, and subsequently losses. On the contrary, the bilinear IM-EDP model increases the median value of total loss estimates by 5% and 11% compared to the linear model in component- and SLF-based, respectively (Figure 6d). The linear relationship underpredicts the maximum floor-level EDP response compared to the bilinear relationship, particularly for top stories, resulting in a lower damage estimation, and seismic losses. As Figure 6e shows, this trend remains the same among all building heights, except for 1-story buildings, where the bilinear model provides lower loss for the SLF-based method, similar to assembly-based approach. Furthermore, unlike component- and SLF-based approaches, the bilinear model exhibits a lower probability of exceeding higher damage states than a linear model for a given IM level (Figure 6f and c). It should be noted that the observed trends are also

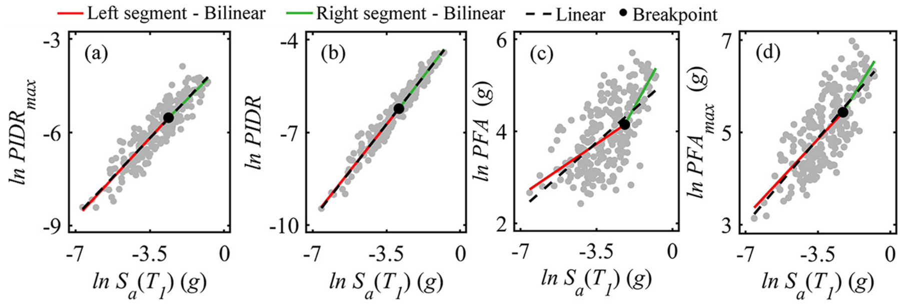

Figure 7. Log-log relationship between (a) $PIDR_{max}$, (b) *PIDR*, (c) PFA_{max}, and (d) *PFA* with respect to $S_a(T_1)$ highlighting the linear and bilinear fitting models.

influenced by the moderate level of nonlinearity exhibited by the analyzed SMRF buildings under the considered GM suite. It is expected that under more strong GM records, the difference between bilinear and linear IM-EDP models increases.

The effect of using different EDP statistics in the assembly-based approach

As discussed in the previous section, the HAZUS assembly-based approach exhibits significant variability in the estimated loss, possibly leading to an inconsistent portfolio assessment. The high variability in the assembly-based method is partially due to using a single building-level EDP statistic (i.e. maximum EDP over the entire building). Therefore, this sensitivity assessment evaluates alternative EDP statistic that can be better correlated to floor-level response distribution, hence improving the assembly-based estimates.

Several candidate EDP statistics were examined, including mean, 75th percentile, 90th percentile, weighted average of mean and maximum ($WA_{Mean-Max}$), weighted average of minimum and maximum ($WA_{Min-Max}$), and weighted average of different EDP percentiles. For weighted average metrics, a weight factor, denoted as α, was introduced to control the contribution of the different EDP statistic in the weighted average formulation. Here, the weights of the weighted average-based metrics were computed through an optimization algorithm to minimize the difference between loss values of assembly- and component-based methods for each building. Since such information does not exist a priori, the calculated α was regressed with respect to an available simple proxy, that is, the buildings' fundamental period (T_1). Figure 8b shows the regression for WA_{25-75}, which can provide a basis to estimate α for WA_{25-75} for other steel moment frame buildings outside of the studied buildings. It should be noted that the estimated α in Figure 8b (and not the exact α) was used in this study. Similar equations were developed for other weighted average-based metrics. Finally, all different calculated EDP statistics were then incorporated into estimating fragility functions, and subsequently loss values, of the assembly-based approach. Table S5 of Supplementary Materials presents the normalized EAL for all the EDP statistics.

Figure 8a shows the normalized total EAL of the assembly-based approach calculated using various EDP statistics and their comparison to component- and SLF-based methods. First, the median of the total loss estimates of assembly-based approach using maximum EDP statistic is similar to the component-based method, whereas the dispersion is significantly higher. In contrast, using mean EDP reduces the dispersion of the loss estimates

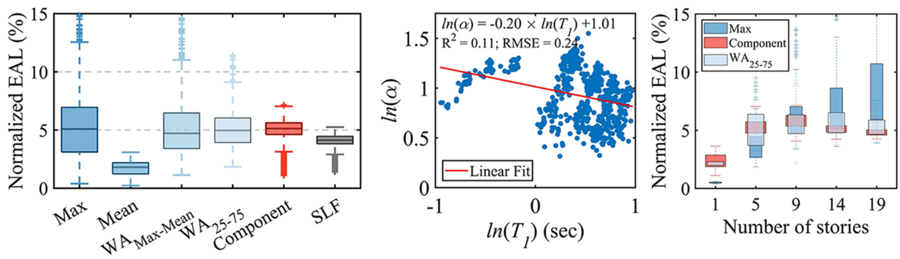

Figure 8. Normalized total EAL (in % of replacement cost) of steel database buildings using different EDP statistics within the assembly-based approach. (a) Comparison of normalized EAL for various EDP statistics (including maximum, mean, weighted average, $WA_{Mean-Max}$ and WA_{25-75}) with component- and SLF-based methods. (b) Linear regression of the logarithm of optimized weight factor ($ln(\alpha)$) against the fundamental period ($ln(T_1)$). (c) Variation of normalized EAL across buildings with different number of stories, highlighting differences between maximum, component-based, and weighted average (WA_{25-75}).

compared to maximum EDP. However, it also substantially increases the difference between the median loss estimates between assembly- and component-based approaches. Second, comparing different weighted average-based statistics, $WA_{Mean-Max}$ slightly reduced the dispersion compared to maximum EDP, while the dispersion is still significantly larger than the component-based method. On the other hand, WA_{25-75} was found to significantly reduce the variability in loss estimate compared to all the other studied EDP statistics while maintaining median loss estimates close to component-based approach. Furthermore, as shown in Figure 8c, the WA_{25-75} yields better median and dispersion of loss estimates across all the building heights compared to conventional maximum EDP response. In summary, WA_{25-75} was found to be a better EDP statistic than the conventional maximum EDP for the studied database, as it reduces estimate dispersion and produces more consistent loss estimates over large building portfolios.

Impact of residual drift on demolition loss

Residual drifts significantly influence seismic loss estimates and often result in the underestimation of these losses if the probability of demolition given RIDR (i.e. $G(D|RIDR)$) is overlooked (Ramirez and Miranda, 2012). Current loss methodologies define $G(D|RIDR)$ using residual drift thresholds characterized based on past empirical data and state of practice (Ramirez and Miranda, 2012). However, limited empirical data exist to support such characterizations over different building systems, resulting in various proposed RIDR thresholds for this distribution. For example, Ramirez and Miranda (2012) used a lognormal distribution of RIDR, assuming a median of 1.5% and a dispersion of 0.3, whereas Iwata et al. (2006) suggested a limit of 1.4% median RIDR for steel buildings. Others have considered thresholds ranging from 0.2% to 2% (FEMA P-58, 2012; Erochko et al., 2011; McCormick et al., 2008). Irrespective of the suggested thresholds, the extent that total loss estimates may vary based on different parametrizations of $G(D|RIDR)$ is unclear. Therefore, the influence of residual drift thresholds and uncertainty on the demolition and total loss of the studied steel buildings is evaluated in this section. First, to investigate the sensitivity of loss estimates to the median of $G(D|RIDR)$, loss assessments were conducted using median values of 0.5%, 1.0%, 1.5%, 2.0%, 2.5%, 3.0%, 5.0%, and at a constant dispersion of 0.30. Next, to explore the sensitivity of loss estimates to the

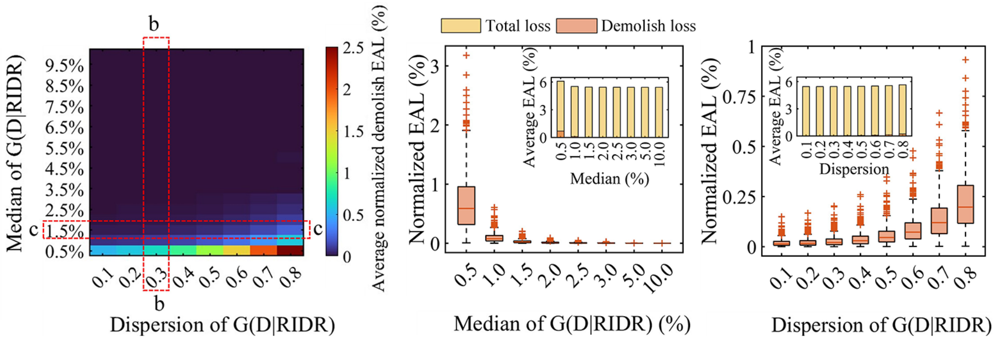

Figure 9. Normalized EAL (in % of replacement cost) to variations in the median and dispersion of residual drift distribution. (a) The heatmap illustrates the variation in average demolition EAL (for entire database steel buildings) across the full parameter space. Subfigures show normalized and average normalized EAL with (b) varying median values at a 0.3 dispersion and (c) varying dispersion values at a fixed 1.5% median.

dispersion of $G(D|RIDR)$, loss estimations were performed with varying dispersion values of 0.1, 0.2, 0.3, 0.4, 0.5, 0.6, 0.7, and 0.8 at the fixed median value of 1.5%.

Figure 9 shows the normalized demolition and total EAL of the studied steel buildings with respect to considered ranges of the median and dispersion values. A two-dimensional sensitivity study was also conducted to explore the combined influence of both the median and dispersion of $G(D|RIDR)$. The resulting heatmap (Figure 9a) shows the average normalized demolish EAL for an entire steel buildings database. Figure 9b shows normalized and average normalized EAL with varying median values at a 0.3 dispersion, and Figure 9c shows varying dispersion values at a fixed 1.5% median.

As shown in Figure 9b, the total EAL reduces as the median values of $G(D|RIDR)$ increases, where the demolition loss contribution significantly decreases and becomes negligible for median residual drift values of greater than 1.5%–2%. These results are similar to previous findings of Ramirez and Miranda (2012) for RC moment frames, albeit the demolition loss contributions are significantly lower for the studied steel moment frames. In contrast, Figure 9c shows no significant effect of residual drift dispersion on total EAL, implying that total loss estimates are more sensitive to the median compared to the dispersion of $G(D|RIDR)$. Moreover, the contribution of demolition loss increases for dispersion values above 0.3, conforming to the observations by Ramirez and Miranda (2012). Figure 9a illustrates dispersion significantly affects demolition losses only when the RIDIR threshold is less than 1.5%, whereas demolition losses become negligible for all dispersion values when the thresholds exceed 1.5%.

Impact of uncertainty in nonstructural quantities

A common modeling decision in loss estimation is to use median component quantities, typically derived from past construction data, using the FEMA P-58 Normative Tool. However, past studies have shown that variations in nonstructural component quantities notably affect repair cost estimates, where buildings with a larger number of these components (categorized as higher luxury levels) have higher repair costs (Papadopoulos et al., 2019). Therefore, this section investigates how uncertainty in nonstructural component

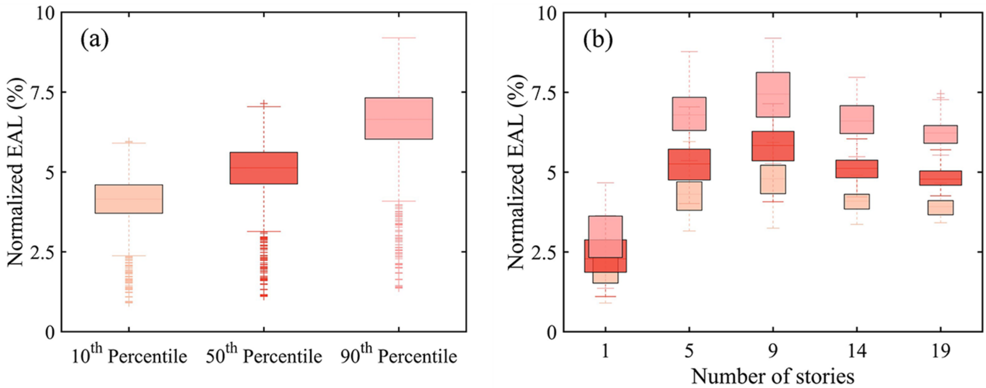

Figure 10. Normalized total EAL (in % of replacement cost) of steel database buildings considering 10th, 50th, and 90th percentile nonstructural quantities in FEMA P-58 component-based approach for (a) entire database (b) variation across buildings with different number of stories.

quantity affects loss estimates. The 10th, 50th, and 90th percentiles were calculated using the data from the normative tool of FEMA P-58, assuming a lognormal assumption.

Figure 10 illustrates the total normalized EAL for considered percentiles for the entire database of steel buildings. Overall, the median loss estimates increase as the nonstructural quantity percentile increases, where using nonstructural quantities corresponding to the 10th percentile resulted in 19% and 16% lower median and dispersion for the total estimated loss. In contrast, adopting a 90th percentile yielded about a 30% increase in both the median and dispersion of the total loss estimate. Furthermore, the impact of nonstructural quantity on median loss was consistent across different building heights. For instance, the difference in median losses between 10th and 50th percentiles, and 50th and 90th percentiles are around 18% to 20% and 26% to 30%, respectively. On the other hand, the effect of nonstructural quantity on dispersion was more pronounced for taller frames at the 90th percentile and for shorter frames at the 10th percentile. For example, using the 90th percentile instead of the 50th percentile for nonstructural component quantities resulted in 51% and 44% increase in 14- and 19-story buildings loss estimates, whereas by reducing the median to the 10th percentile, the dispersion of total loss for 1-story was decreased by 22%.

Discussion of results and recommendations

The presented comparative analysis and corresponding sensitivity aim to answer two research questions: (1) *how do the estimates from different loss methodologies change over different building taxonomies?* and (2) *Which modeling decision affects these differences more?* To answer the first question, Figure 5 can be further scrutinized. Overall, SLF- and component-based results are mostly similar over all loss types, except for structural loss. In contrast, assembly-based and component-based results are mostly different, except for 1-story buildings, and when comparing structural loss. Despite the notable difference between the assembly-based approach and other methods in loss estimates for buildings with varying heights, from a portfolio-level assessment perspective, these methods provide similar mean loss estimates. For example, the assembly-based approach only has 0.8% lower values than component-based methods when considering the entire building

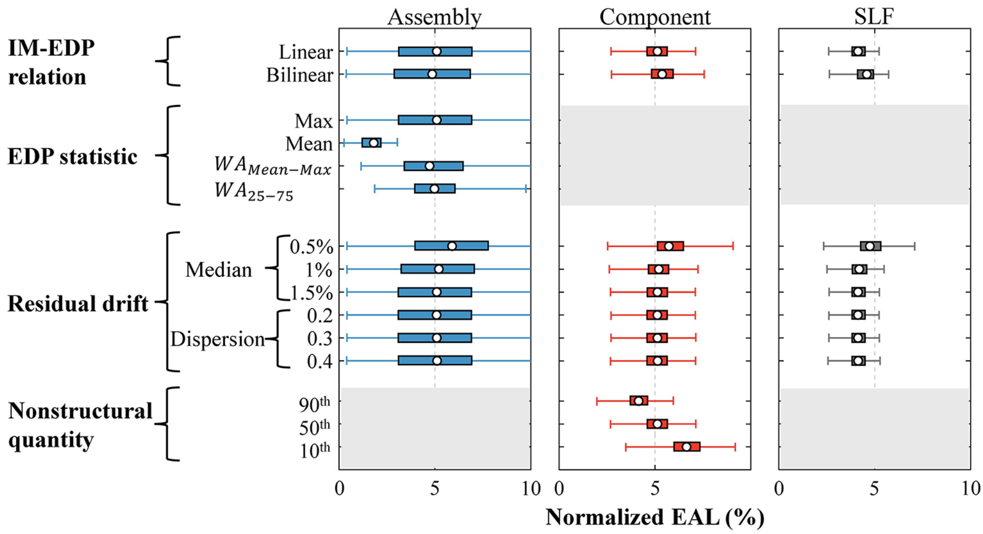

Figure 11. Comparison of various sensitivity parameters for assembly-, component-, and SLF-based methods with respect to normalized total EAL (in % of replacement cost) of steel database buildings. Shaded areas show the space where sensitivity did not apply to the considered methodology.

database. This observation is to the distribution of building topologies (i.e. the larger number of short- and medium-rise buildings in the studied database). In contrast, the SLF-based approach provides the lowest estimate of total EAL over the entire database, showing 20% lower median estimates than the component-based approach. In summary, using the assembly-based approach is recommended when analyzing short and medium-rise buildings, or when the inventory consists of only a few tall buildings. The analysts should be aware that those estimates, even for shorter buildings, have high variability, which could propagate more errors into the assessment.

To answer the second question, Figure 11 compares the relative impact of considered analysis decisions on seismic loss estimates across different methodologies, aiming to determine which modeling choices have the highest impact. In the assembly-based method, EDP statistics have the largest impact on total EAL among considered decisions. While the maximum EDP and WA_{25-75} statistic yields similar median EAL, WA_{25-75} reduces the dispersion by 49% compared to the conventional maximum EDP. In addition, the IM-EDP relationship has a moderate effect, with the bilinear model slightly reducing the median EAL by 5% with similar dispersion EAL. Overall, to reduce the difference between assembly-based and component-based approaches, the analysis should focus on at least performing loss assessment with EDP statistics that better capture EDP variations over floors than a conservatively high value of maximum. For the studied building, using the weighted average of EDP percentiles (than the conventional maximum value) reduced the difference between the total losses from assembly- and component-based approaches.

For the component-based method, the choice of nonstructural quantity is the most important factor that affects the loss estimates among the considered decisions. Increasing the nonstructural quantity from 10th to the 90th percentile causes a 62% increase in the median EAL and a 55% rise in dispersion, demonstrating that higher nonstructural quantities contribute to both greater loss estimates and variability. The IM-EDP relationship has a moderate impact, with the bilinear model slightly increasing the median EAL by 5% while reducing the dispersion by 8%. Therefore, to improve the accuracy of estimates, it is recommended that a detailed inventory of nonstructural would be used, as using crude central measure-based data result in significantly different estimates. Current efforts in developing databases of nonstructural components could aid with constructing such inventories for loss assessment of typical constructions (Cook, 2025).

In the SLF-based method, the IM-EDP relationship formulation has the highest impact, where a bilinear formulation significantly affects both the magnitude and variability of loss estimates. Finally, dispersion RIDR has no significant impact on both the median and dispersion of EAL. Therefore, to improve the accuracy of SLF estimates, it is recommended that the underlying SLFs are derived using more refined IM-EDP formulations, possibly through methods that can better capture the nonlinearity.

Finally, across all methods, the residual drift thresholds primarily affect the median EAL, with higher RIDR thresholds reducing median EAL, while RIDR dispersion does not notably affect the total loss estimates. In the assembly-based approach, the median EAL decreases by 14% as the RIDR thresholds increase from 0.5% to 1.5%, whereas this reduction changes to 11% and 13% in component- and SLF-based methods. Therefore, following a conservative approach, lower RIDR thresholds may be used to avoid underpredicting medial total losses.

Conclusion

Summary

This study presented a comprehensive comparison of seismic loss estimation methodologies with varying fidelity, namely, HAZUS assembly-based, FEMA P-58 component-based, and SLF-based approaches over a database of 621 SMRF buildings. The SMRF building covers a wide range of building topologies and designs, ranging from 1-story to 19-story buildings. In addition, this study investigated the sensitivity of seismic loss estimates to four different analysis decisions at the fragility and loss assessment stages that are often left to the analyst's judgment. Specifically, the impact of different mathematical formulations for IM-EDP relationships (i.e. linear and bilinear models), EDP representation in damage models in the assembly-based approach, residual drift (RIDR) distribution, and uncertainty in the nonstructural quantities. The following conclusions summarize the main findings of this study regarding the comparison of different methodologies:

1. Among different methods, the assembly-based approach provides lower median total loss estimates for short- to medium-rise buildings, and higher estimates for taller buildings compared to the component-based method, respectively.
2. The total loss estimates from the assembly-based approach show significantly higher variability than the component-based method for multi-story buildings (i.e. 3 times higher over the entire inventory).
3. The SLF-based method provides slightly higher median total loss estimates (i.e. 0.4%) for 1-story buildings and consistently lower estimates (i.e. on average, 16%) for multi-story buildings than the component-based method.

The main findings of sensitivity assessments are summarized as follows:

1. Using a bilinear IM-EDP model in the assembly-based approach reduces the median total loss estimates by 5% compared to a linear model. In contrast, the bilinear model increases median estimates by 5% and 11% in the component- and SLF-based methods, respectively.
2. Incorporating the weighted average of 25th and 75th percentile EDPs (as opposed to the conventional maximum value) in the assembly-based approach substantially reduces the variability of total loss estimates while maintaining median losses comparable to the component-based method.
3. The contribution of demolition loss significantly decreases for RIDR threshold values greater than 1.5%–2% and increases when the dispersion of RIDR values is more than 30%, conforming to observations by Ramirez and Miranda (2012) for concrete frame buildings. In addition, the dispersion significantly affects demolition losses only when the median is below 1.5%, whereas demolition losses become negligible regardless of dispersion when the median exceeds 1.5%.
4. Across all loss methods, sensitivity to median RIDR primarily affects median loss estimates with minimal impact on the dispersion of loss estimates, while the dispersion of RIDR does not have a significant impact on the loss estimates in the analyzed scenarios.
5. The impact of nonstructural quantity on median loss estimates is consistent across all buildings' heights. Nevertheless, the effect on dispersion loss estimates is mostly notable in taller buildings (14- and 19-story) at 90th percentile quantity and in shorter buildings (1-story) at 10th percentile quantity values.
6. Comparing the relative importance of different analysis decisions shows that the most critical choice varies by methodology. Among the considered factors, the choice of EDP statistics is the most influential factor affecting the dispersion of loss estimates for the assembly-based approach, whereas nonstructural component quantity estimates govern both the median and dispersion of loss estimates in the component-based method. The formulation of the IM-EDP relationship was found to have the highest impact for the SLF-based method and second most important in assembly- and component-based methods.

Limitations and future work

The results of this study are constrained to a steel SMRF planar frame database. Future work is needed to extend the scope of such benchmarking studies to a more diverse set of buildings, including various lateral systems (e.g. steel, RC, and masonry frames), different soil conditions, and geographic locations with different seismic hazards. In addition, this study focused on decisions beyond hazard and GM/IM selection, and hence followed the practice of using an unscaled suite of GMs for inventory-level assessment. However, to ensure hazard-consistency and a broader range of nonlinear behavior, each GM should be scaled to the target spectra based on the site's hazard. Future studies are needed to study the effect of scaling GMs on the estimates from different loss methods.

Further research is also needed to determine appropriate statistical parameters for the demolition distribution of steel buildings. This can be achieved by collecting post-earthquake data for steel buildings to develop accurate demolition probability models. In addition, the computation of residual drifts in this study does not account for the sensitivity of predictions to hysteretic behavior, degradation models, P-Delta effects, and free vibration response. These modeling aspects significantly influence residual drift predictions and should be considered in future studies.

Due to the unavailability of construction data, this study ignored the effect of market conditions, location, and labor rates that could affect cost data. For example, the consequence functions reported in the FEMA P-58 component-based method were specific to Northern California in 2011. In addition, the normative tool of FEMA P-58 does not provide nonstructural components related to building content (e.g. workstations, printers, desks, and cabinets), which contribute to nonstructural losses in office occupancy. Future studies should include region-specific cost data and consider the variability in repair and replacement costs to enhance the accuracy of loss estimates.

Declaration of conflicting interests

The author(s) declared no potential conflicts of interest with respect to the research, authorship, and/or publication of this article.

Funding

The author(s) received no financial support for the research, authorship, and/or publication of this article.

ORCID iDs

Shivalinga Baddipalli https://orcid.org/0000-0003-0597-8166
Roberto Gentile https://orcid.org/0000-0002-7682-4490
Gerard J. O' Reilly https://orcid.org/0000-0001-5497-030X
Davit Shahnazaryan https://orcid.org/0000-0002-0529-5763
Mohsen Zaker Esteghamati https://orcid.org/0000-0002-2144-2938

Data and resources

All data and codes used in this study will become publicly available on GitHub at https://github.com/StoStruct/Loss_Comparison_Paper (https://doi.org/10.5281/zenodo.15764906)

Supplemental material

Supplemental material for this article is available online.

References

Baker JW and Cornell CA (2008) Uncertainty propagation in probabilistic seismic loss estimation. *Structural Safety* 30(3): 236–252.

Calvi GM, Pinho R, Magenes G, Bommer JJ, Restrepo-Vélez LF and Crowley H (2006) Development of seismic vulnerability assessment methodologies over the past 30 years. *ISET Journal of Earthquake Technology* 43(3): 75–104.

Cook D (2025) *Ned-Beta: Nonstructural Element Database* (Version Beta) (NIST). U.S. National Institute of Standards and Technology. https://github.com/usnistgov/NED

Cornell CA and Krawinkler H (2000) Progress and challenges in seismic performance assessment. *PEER Newsletter*. https://apps.peer.berkeley.edu/news/2000spring/performance.html (accessed 5 August 2025).

Cremen G and Baker JW (2021) Variance-based sensitivity analyses and uncertainty quantification for FEMA P-58 consequence predictions. *Earthquake Engineering & Structural Dynamics* 50(3): 811–830.

Crowley H, Bommer JJ, Pinho R and Bird J (2005) The impact of epistemic uncertainty on an earthquake loss model. *Earthquake Engineering & Structural Dynamics* 34(14): 1653–1685.

Dyanati M, Huang Q and Roke D (2017) Sensitivity analysis of seismic performance assessment and consequent impacts on loss analysis. *Bulletin of Earthquake Engineering* 15(11): 4751–4790.

Erochko J, Christopoulos C, Tremblay R and Choi H (2011) Residual drift response of SMRFs and BRB frames in steel buildings designed according to ASCE 7-05. Journal of Structural Engineering 137(5): 589–599.

Esteghamati MZ and Farzampour A (2020) Probabilistic seismic performance and loss evaluation of a multi-story steel building equipped with butterfly-shaped fuses. *Journal of Constructional Steel Research* 172: 106187.

Esteghamati MZ and Flint MM (2021) Developing data-driven surrogate models for holistic performance-based assessment of mid-rise frame buildings at early design. *Engineering Structures* 245: 112971.

Esteghamati MZ, Rodriguez-Marek A and Flint MM (2023) A reliability-based decision support system for resilient and sustainable early design. In *Resilient and Sustainable Buildings*. Reston, VA: American Society of Civil Engineers, pp. 177–228.

Federal Emergency Management Agency (FEMA) (1999) *HAZUS-MH: Multi-Hazard Loss Estimation Methodology*. Washington, DC: Technical Manual.

FEMA. FEMA P-58-1 (2012): Seismic Performance Assessment of Buildings. Volume 1–Methodology. Washington, DC: Federal Emergency Management Agency.

FEMA, P-58-1 (2018) *Seismic Performance Assessment of Buildings*. Volume 1–Methodology. Redwood City, CA: Applied Technology Council.

FEMA, P-58-3 (2018) *Seismic Performance Assessment of Buildings*. Volume 3–Supporting Electronic Materials and Background Documentation, Third Edition. Redwood City, CA: Applied Technology Council.[AQ: 13]

Freddi F, Padgett JE and Dall'Asta A (2017) Probabilistic seismic demand modeling of local level response parameters of an RC frame. *Bulletin of Earthquake Engineering* 15: 1–23.

Frucht E, Salamon A, Rozelle J, Levi T, Calvo R, Avirav V and Bausch D (2021) Tsunami loss assessment based on Hazus approach–The Bat Galim, Israel, case study. *Engineering Geology* 289: 106175.

Gentile R and Galasso C (2021) Accounting for directivity-induced pulse-like ground motions in building portfolio loss assessment. *Bulletin of Earthquake Engineering* 19(15): 6303–6328.[AQ: 14]

Guan M, EERI X, Burton M, EERI H and Shokrabadi M (2021) A database of seismic designs, nonlinear models, and seismic responses for steel moment-resisting frame buildings. *Earthquake Spectra* 37(2): 1199–1222.

Gupta A and Krawinkler H (1999) *Seismic demands for performance evaluation of steel moment resisting frame structures (Report No.132)*. John A. Blume Earthquake Engineering Center, Department of Civil Engineering, Stanford University.

HAZUS-MH 2.1. (2015) *Earthquake Model Technical Manual*. Washington, DC: Federal Emergency Management Agency.[AQ: 15]

Hwang SH and Lignos DG (2017) Earthquake-induced loss assessment of steel frame buildings with special moment frames designed in highly seismic regions. *Earthquake Engineering & Structural Dynamics* 46(13): 2141–2162.

Hwang SH, Jeon JS and Lee K (2019) Evaluation of economic losses and collapse safety of steel moment frame buildings designed for risk categories II and IV. *Engineering Structures* 201: 109830.

Ibarra LF and Krawinkler H (2005) *Global Collapse of Frame Structures Under Seismic Excitations*. Berkeley, CA: Pacific Earthquake Engineering Research Center.

Ibarra LF, Medina RA and Krawinkler H (2005) Hysteretic models that incorporate strength and stiffness deterioration. *Earthquake Engineering & Structural Dynamics* 34(12): 1489–1511.

Iwata Y, Sugimoto K and Kuwamura H (2006) Reparability limit of steel structural buildings based on the actual data of the HyogokenNanbu earthquake. In: *Wind and Seismic Effects: Proceedings of the 38th Joint Panel on Wind and Seismic Effects*, NIST Special Publication 1057, pp. 23–32.

Jalayer F and Cornell CA (2009) Alternative non-linear demand estimation methods for probability-based seismic assessments. *Earthquake Engineering & Structural Dynamics* 38(8): 951–972.[AQ: 16]

Kijewski-Correa T, Cetiner B, Zhong K, Wang C, Zsarnoczay A, Guo Y and McKenna F (2023) Validation of an augmented parcel approach for hurricane regional loss assessments. *Natural Hazards Review* 24(3): 04023022.

Kircher CA, Nassar AA, Kustu O and Holmes WT (1997) Development of building damage functions for earthquake loss estimation. *Earthquake Spectra* 13(4): 663–682.

Kircher CA, Whitman RV and Holmes WT (2006) HAZUS earthquake loss estimation methods. *Natural Hazards Review* 7(2): 45–59.

Krawinkler H (1978) Shear in beam-column joints in seismic design of steel frames. *Engineering Journal* 15(3): 82–91.

Lamprou A, Jia G and Taflanidis AA (2013) Life-cycle seismic loss estimation and global sensitivity analysis based on stochastic ground motion modeling. *Engineering Structures* 54: 192–206.

Lignos D (2008) *Sidesway collapse of deteriorating structural systems under seismic excitations*. Phd Thesis, Stanford University, Stanford, CA.

Lignos DG and Krawinkler H (2011) Deterioration modeling of steel components in support of collapse prediction of steel moment frames under earthquake loading. *Journal of Structural Engineering* 137(11): 1291–1302.

McCormick J, Aburano H, Ikenaga M and Nakashima M (2008) Permissible residual deformation levels for building structures considering both safety and human elements. In: *14th World Conference on Earthquake Engineering*, Paper No. 05-06-0071. Beijing, China.

McKenna F, Fenves GL, Scott MH and Jeremic B (2000) *Open System for Earthquake Engineering Simulation (OpenSees)*. Berkeley, CA: Pacific Earthquake Engineering Research Center, University of California.

Miranda E (2000) Inelastic displacement ratios for structures on firm sites. *Journal of Structural Engineering* 126(10): 1150–1159.

O'Reilly GJ and Calvi GM (2019) Conceptual seismic design in performance-based earthquake engineering. *Earthquake Engineering & Structural Dynamics* 48(4): 389–411.

O'Reilly GJ and Monteiro R (2019) Probabilistic models for structures with bilinear demand-intensity relationships. *Earthquake Engineering & Structural Dynamics* 48(2): 253–268.

O'Reilly GJ and Shahnazaryan D (2024) On the utility of story loss functions for regional seismic vulnerability modeling and risk assessment. *Earthquake Spectra* 40(3): 1933–1955.

Papadopoulos AN, Vamvatsikos D and Kazantzi AK (2019) Development and application of FEMA P-58 compatible story loss functions. *Earthquake Spectra* 35(1): 95–112.

Porter K, Farokhnia K, Vamvatsikos D and Cho I (2015) *Guidelines for Component-Based Analytical Vulnerability Assessment of Buildings and Nonstructural Elements*. Boulder, CO: Global Vulnerability Consortium.

Porter KA, Beck JL and Shaikhutdinov RV (2002) Sensitivity of building loss estimates to major uncertain variables. *Earthquake Spectra* 18(4): 719–743.

Ramirez CM and Miranda E (2012) Significance of residual drifts in building earthquake loss estimation. *Earthquake Engineering & Structural Dynamics* 41(11): 1477–1493.

Ramirez CM, Liel AB, Mitrani-Reiser J, Haselton CB, Spear AD, Steiner J and Miranda E (2012) Expected earthquake damage and repair costs in reinforced concrete frame buildings. *Earthquake Engineering & Structural Dynamics* 41(11): 1455–1475.

Scawthorn C, Flores P, Blais N, Seligson H, Tate E, Chang S and Lawrence M (2006) HAZUS-MH flood loss estimation methodology. II. Damage and loss assessment. *Natural Hazards Review* 7(2): 72–81.

Schneider PJ and Schauer BA (2006) HAZUS—Its development and its future. *Natural Hazards Review* 7(2): 40–44.

Shahnazaryan D and O'Reilly GJ (2021) Integrating expected loss and collapse risk in performance-based seismic design of structures. *Bulletin of Earthquake Engineering* 19(2): 987–1025.

Shahnazaryan D, O'Reilly GJ and Monteiro R (2021) Story loss functions for seismic design and assessment: Development of tools and application. *Earthquake Spectra* 37(4): 2813–2839.

Silva A, Castro JM and Monteiro R (2020) Brace-to-frame connection modelling effects on seismic loss assessment of steel concentrically-braced frames. *Journal of Constructional Steel Research* 172: 106230.

Silva V, Akkar S, Baker J, Bazzurro P, Castro JM, Crowley H and Vamvatsikos D (2019) Current challenges and future trends in analytical fragility and vulnerability modeling. *Earthquake Spectra* 35(4): 1927–1952.
Terzic V, Merrifield SK and Mahin SA (2012) Lifecycle cost comparisons for different structural systems designed for the same location systems designed for the same location. In: *15th world conference on earthquake engineering*. Lisbon, Portugal.
Tubaldi E, Freddi F and Barbato M (2016) Probabilistic seismic demand model for pounding risk assessment. *Earthquake Engineering & Structural Dynamics* 45(11): 1743–1758.
United States Geological Survey (2023) Unified Hazard Tool. Available at: https://earthquake.usgs.gov/hazards/interactive (accessed 26 February 2025).
Welch DP, Sullivan TJ and Calvi GM (2014) Developing direct displacement-based procedures for simplified loss assessment in performance-based earthquake engineering. *Journal of Earthquake Engineering* 18(2): 290–322.
Whitman RV, Anagnos T, Kircher CA, Lagorio HJ, Lawson RS and Schneider P (1997) Development of a national earthquake loss estimation methodology. *Earthquake Spectra* 13(4): 643–661.
Zaker Esteghamati M (2022) A holistic review of GM/IM selection methods from a structural performance-based perspective. *Sustainability* 14(20): 12994.

Appendix 1

Loss analsis formulations

FEMA P-58 component-based approach: In this approach, the expected total seismic losses are disaggregated into three possible scenarios: (1) the building does not collapse (*NC*), but structural and nonstructural components need repair (*R*), $NC \cap R$; (2) the building does not collapse, but due to excessive residual deformations, it needs to be demolished (*D*) and rebuilt, $NC \cap D$; and (3) building collapses (*C*) and must be rebuilt. Since these scenarios are mutually exclusive and collectively exhaustive, the expected total losses conditioned on intensity measure (*IM*) are computed using the total probability theorem as follows:

$$E[L_T|IM] = E[L_T|NC \cap R, IM] \cdot \{1 - P(D|NC, IM)\} \cdot \{1 - P(C|IM)\} + E[L_T|NC \cap D, IM] \cdot P(D|NC, IM) \cdot \{1 - P(C|IM)\} + E[L_T|C, IM] \cdot P(C|IM) \quad \text{(A.1)}$$

where $E[L_T|IM]$ is the expected total loss (L_T) conditioned on a given value of IM. The expected demolition loss, $E[L_T|NC \cap D, IM]$, is assumed equal to the total replacement cost plus the cost due to building demolition, which is considered to be 10% of the total replacement cost (Hwang and Lignos, 2017). $P(D|NC, IM)$ is the probability of a building not collapsing but requiring demolition for a given IM. $P(C|IM)$ denotes the probability of the building collapsing for a given IM. No collapse records observed in the database buildings, thus, collapse cases are not included in the study. Here, the expected non-collapse loss, $E[L_T|NC \cap R, IM]$, is evaluated using the following equation:

$$E[L_T|NC \cap R, IM] = \sum_{k=1}^{s} \sum_{i=1}^{m} \sum_{j=1}^{n} \int_{0}^{\infty} E(L_{ij}|DS_{ij}) P(DS_{ij}|EDP_k) f(EDP_k|IM) dEDP_k \quad \text{(A.2)}$$

where m is the number of components considered in the story, n is the number of damage states for each component, and s is the number of stories. $f(EDP_k|IM)$ represents the probability density function of EDP at the kth floor (i.e. EDP_k) given IM, which is assumed to follow a lognormal distribution. The median and dispersion of $f(EDP_k|IM)$ distribution are obtained by performing a regression on the cloud of the logarithmic values of EDP_k against the corresponding IM values (Jalayer and Cornell, 2009; Gentile and Galasso, 2021). Each IM and its associated EDP are treated individually for integration in Equation (A.2). To ensure a comprehensive loss assessment across varying seismic intensities, a continuous range of IM values (0 to 2 g in 0.01 g increments) was input into the regression model to predict the corresponding EDP_k distributions (median and dispersion). For each IM value, the corresponding EDP distributions were utilized to compute losses individually at the component level by applying fragility and consequence functions through Equation (A.2). The computed component-level losses were aggregated at the story level and subsequently summed across all floors to obtain the total building-level seismic loss for each IM value within the considered range.

In Equation (A.2), $E(L_{ij}|DS_{ij})$ is the median repair cost of ith component at the jth damage state. $P(DS_{ij}|EDP_k)$ characterizes the probability of ith component being at the jth damage state given EDP_k and computed following a lognormal cumulative distribution function. The median and dispersion EDP demand of ith component corresponding to a jth damage state of $P(DS_{ij}|EDP_k)$ distribution are determined using fragility functions P-58. Moreover, in Equation (A.1), the probability of a building being demolished at a given IM, $P(D|NC, IM)$ is computed following Ramirez and Miranda (2012). The lognormal probability distribution, $G(D|RIDR)$, of building demolition conditioned on maximum RIDR among all the stories is calculated by assuming 1.5% median and 0.3 dispersion of $G(D|RIDR)$. It's worth highlighting that $P(D|NC, IM)$ and expected demolition loss is calculated using a similar approach in assembly- and SLF-based methods as well.

HAZUS assembly-based approach: The median and standard deviation of the prediction is obtained to characterize $f(EDP|IM)$. Here, Equation (A.2) is adjusted as follows:

$$E[L_T|NC \cap R, IM] = \sum_{i=1}^{a}\sum_{j=1}^{n}\int_{0}^{\infty} E(L_{aj}|DS_{aj})P(DS_{aj}|EDP)f(EDP|IM)dEDP \tag{A.3}$$

where a and n are the number of assemblies considered in the building and the number of damage states of each assembly, respectively, and $E(L_{aj}|DS_{aj})$ shows the expected repair cost of ath assembly at the jth damage state. $P(DS_{aj}|EDP)$ is the probability of ith assemby being at the jth damage state given EDP and follows a lognormal cumulative distribution function.

Story loss functions (SLFs): Using the SLFs developed for each assembly, the seismic loss estimation is carried out as follows:

$$\lambda(DV) = \int_{IM}\int_{EDP} G(DV|EDP)\, dG(EDP|IM)d\lambda(IM) \tag{A.4}$$

where $G(DV|EDP)$ represents the developed SLFs and DV is decision variable (direct repair cost loss).